Ultra-fine Co nanoparticles *in-situ* anchored on porous conductive nanosheets as efficient electrocatalysts for promoting sulfur redox reaction kinetics

Siyu Wu [a], Xiang Li [a], Qinghua Guan [b], Xin Zhang [a], Yongzheng Zhang [a,c,*], Jian Wang [b,d], Chunyin Shen [a], Hongzhen Lin [b], Yanli Wang [a], Liang Zhan [a,*]

[a] *State Key Laboratory of Chemical Engineering, East China University of Science and Technology, 130 Meilong Road, Shanghai 200237, China*
[b] *i-Lab & CAS Key Laboratory of Nanophotonic Materials and Devices, Suzhou Institute of Nano-tech and Nano-bionics, Chinese Academy of Sciences, Suzhou 215123, China*
[c] *Key Laboratory of Specially Functional Polymeric Materials and Related Technology (Ministry of Education), East China University of Science and Technology, 130 Meilong Road, Shanghai 200237, China*
[d] *Helmholtz Institute Ulm (HIU), Ulm D89081, Germany*

Keywords:
Lithium sulfur battery
Electrocatalysts
Sulfur redox reaction
Co/N co-doping
Mesoporous carbon nanosheet

A B S T R A C T

Lithium-sulfur (Li-S) batteries are considered as one of the most promising energy storage devices due to their high theoretical energy density. However, the sluggish conversion kinetics and the polysulfides shuttling cause terrible capacity attenuation, impeding the practical developments. Herein, the Co/N co-doped mesoporous carbon nanosheet is developed after the pyrolysis of metal organic framework on graphene oxide layer, which is further explored as kinetics promotor towards advanced Li-S batteries. In this structure, the mesoporous carbon nanosheets with large specific surface area serve as the polysulfide trappers by physical constraint and the ultra-fine Co nanoparticles provide chemical adsorption and electrocatalytic capability for polysulfides, thus effectively suppressing the shuttle effect and accelerating the reaction kinetics. As a result, the Li-S batteries with modified kinetic modulation separators exhibit a high capacity of 585.3 mAh g^{-1} after 500 cycles at 1.0 C and excellent rate capability (511.2 mAh g^{-1} at 3 C).

1. Introduction

With the growing demand for high energy density ranging from portable electronic devices to electric vehicles, it is imperative to explore new energy storage systems to compensate for the low energy density of current lithium-ion batteries. Lithium-sulfur (Li-S) batteries have attracted wide attentions due to their ultra-high energy capacity, environmental friendliness and low cost [1,2]. However, the commercialization of Li-S batteries has been hampered by the low conductivity of sulfur, the large volume changes during the charge–discharge processes, and the shuttle effect of soluble lithium polysulfides (LiPSs) [3–5].

To solve these difficulties, many strategies have been tried, including designing conductive sulfur host, modifying the separator and protecting the lithium anode [6–9]. Among which, the modified separators exhibit the prominent advantages, due to their ability to physically block the LiPSs detached from cathode and reactive them. In this case, various functional materials have been coated on the separators and achieved impressive achievements. However, ideal coating layers should satisfy the functions of both conductivity, chemisorption and high catalytic conversion, thus enabling to fulfill high performances Li-S batteries.

Herein, we reported a 2D mesoporous carbon nanosheet with uniformly dispersed Co nanoparticles (ZG@Co) as a kinetics accelerator on the separator for Li-S batteries, which integrates the merits of high conductivity for electron transfer and enriches more active sites for polysulfide conversions. Specifically, the mesoporous carbon nanosheet acts as physical trapper for LiPSs and the Co nanoparticles interact with LiPSs by strong chemical bonds. Therefore, Li-S batteries with ZG@Co modified separators exhibit outstanding cycling and rate performances.

* Corresponding authors at: State Key Laboratory of Chemical Engineering, East China University of Science and Technology, 130 Meilong Road, Shanghai 200237, China (Y. Zhang and L. Zhan).
E-mail addresses: zhangyongzheng@ecust.edu.cn (Y. Zhang), jian.wang@kit.edu (J. Wang), zhanliang@ecust.edu.cn (L. Zhan).

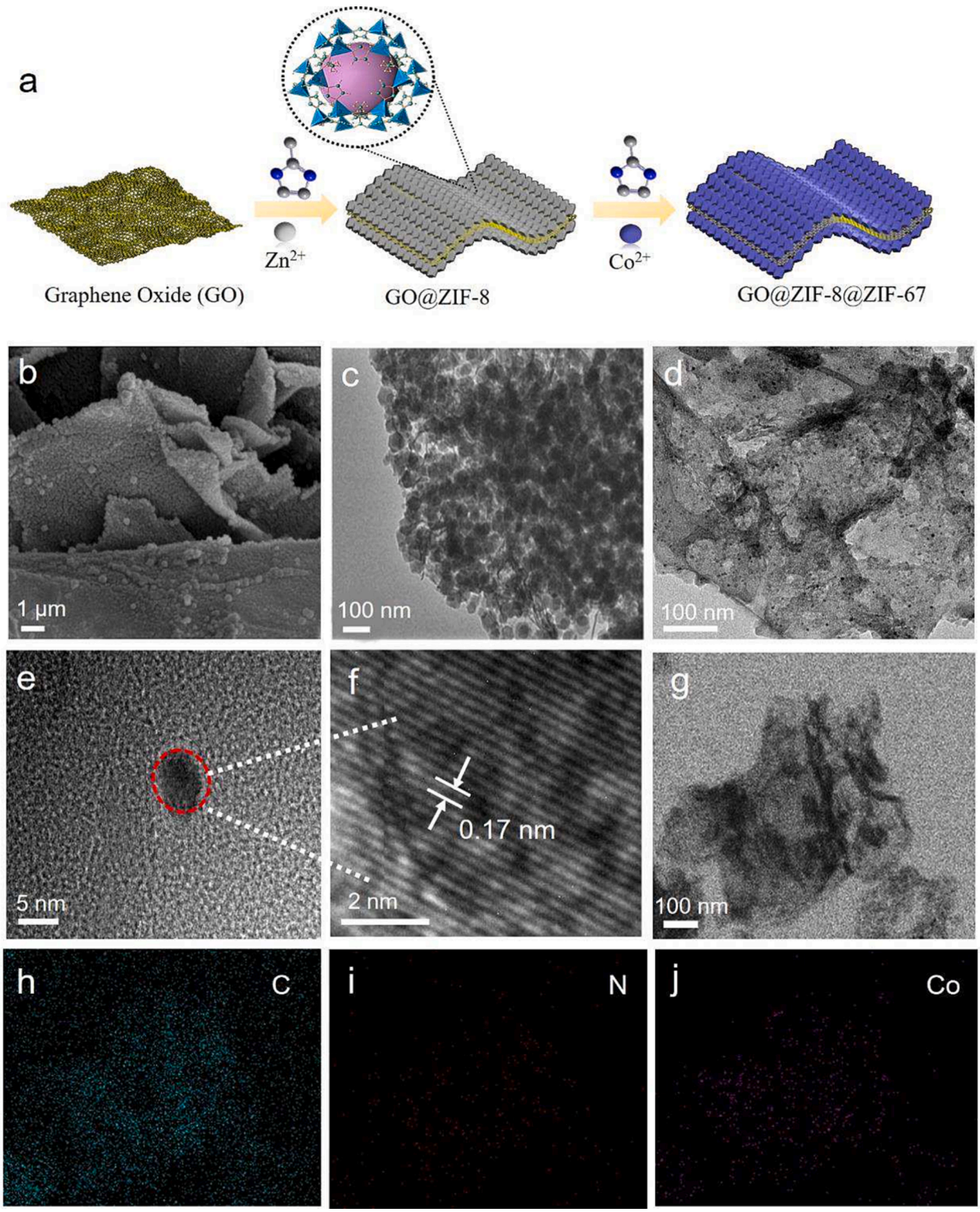

Fig. 1. (a) Schematic illustration preparation process of ZG@Co composites. (b) SEM image of GO@ZIF-8@ZIF-67. TEM images of (c) GO@ZIF-8@ZIF-67 and (d) ZG@Co. (e-f) HRTEM image of ZG@Co and lattice spacing profiles at the selected area framed in red circle. (g-j) STEM image of ZG@Co and corresponding elemental mappings of C, N and Co.

2. Materials and methods

2.1. Synthesis of GO@ZIF-8 and GO@ZIF-8@ZIF-67

Firstly, 0.58 g $Zn(NO_3)_2{\cdot}6H_2O$ was dissolved into 45 mL methanol, and then GO (15 mg) were added. After ultrasonicating for 1 h, 0.66 g 2-methylimidazole dissolved in 50 mL methanol was added and stirred for 30 min to get a homogeneous solution at room temperature. After being aged for 24 h, the product was collected by centrifugation with deionized water. Finally, the GO@ZIF-8 were obtained by vacuum-drying.

0.22 g $Co(NO_3)_2{\cdot}6H_2O$ dissolved in 15 mL methanol was added into 30 mL methanol solution containing 0.3 g GO@ZIF-8 and stirred for 5

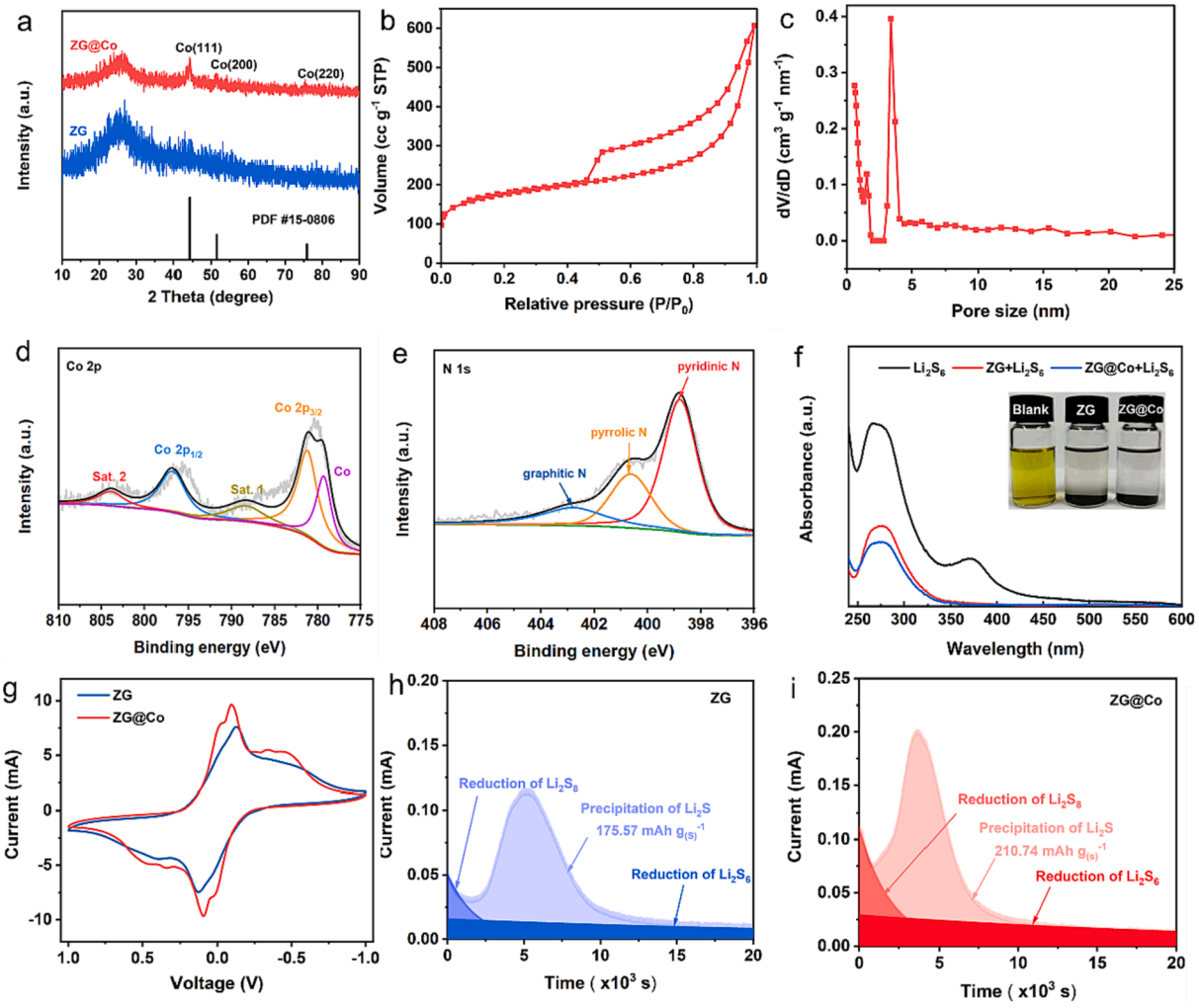

Fig. 2. (a) XRD patterns of ZG and ZG@Co. (b) Nitrogen adsorption isotherm and (c) pore size distribution of ZG@Co. (d) High-resolution spectra of Co 2p and (e) N 1s. (f) Static Li_2S_6 adsorption by ZG and ZG@Co (inset) with the corresponding UV–vis spectra. (g) CV curves with symmetric cell at 5 mV s^{-1}. Li_2S deposition profiles on (h) ZG and (i) ZG@Co.

min. Then, 0.25 g 2-metylimidazole dissolved in 15 mL methanol was added and stirred for 15 min. The product was washed with methanol for three times and dried at 60 °C for 12 h.

2.2. *Synthesis of ZG and ZG@Co*

ZG and ZG@Co was prepared by pyrolysis GO@ZIF-8 and GO@ZIF-8@ZIF-67 at 800 °C for 5 h under N_2 atmosphere.

3. Results and discussion

As illustrated in Fig. 1a, ZIF-8 and ZIF-67 were gradually grown on GO nanosheets to obtain the GO@ZIF-8@ZIF-67 composite. Briefly, Zn^{2+} was adsorbed on GO nanosheet by electrostatic interaction, which was *in-situ* nucleated with 2-methylimidazole to form GO@ZIF-8. Then, ZIF-67 was deposited on ZIF-8 to form GO@ZIF-8@ZIF-67. After calcination, Zn evaporates at high temperature, leaving the pores. Finally, the Co/N co-doped 2D mesoporous carbon sheet (ZG@Co) was obtained. As displayed in Fig. 1b, c, ZIF-8@ZIF-67 particles are uniformly distributed on GO layer. The obtained ZG@Co still retains 2D morphology (Fig. 1d) and the ultra-fine Co nanoparticles with a diameter of 5.88 nm are loaded on nanosheets (Fig. 1d). The high-resolution transmission eletronic microspcope (HRTEM) images in Fig. 1e, f reveal the nanocrystals with a lattice space of 0.17 nm, confirming the highly crystalline property of Co (200). Furthermore, the element mapping results (Fig. 1g–j) also confirm the C, N and Co elements are uniformly distributed in ZG@Co.

Additionally, the crystal structure and the pore structure were further studied. As shown in Fig. 2a, new characteristic peaks can be observed in ZG@Co compared with pure ZG, which well matches with metallic Co (JCPDS No.15–0806). Furthermore, nitrogen absorption–desorption isotherms (Fig. 2b, c and Fig. S1) reveal the co-existence of mesopores and micropores concentrated between 1 and 4 nm, which are caused by the volatilization of Zn. In contrast, the ZG@Co exhibits a specific surface area of 633 m^2 g^{-1}, much larger than that of ZG (348 m^2 g^{-1}). The monodisperse Co nanoparticles on GO supported carbon with large specific surface could improve the adsorption capacity and conversion efficiency of polysulfides.

X-ray photoelectronic spectroscopy (XPS) was further used to determine the chemical surroundings of ZG@Co (Fig. 2d, e). The high-solution XPS spectrum of Co 2p can be fitted with five peaks, where the peaks at 781.2 eV and 796.8 eV are attributed to Co $2p_{3/2}$, Co $2p_{1/2}$, and their corresponding satellite structures (Sat.1 and Sat.2) at 788.3 eV and 798.2 eV, respectively [10]. The peak at 779.3 eV corresponds to Co [11]. The XPS spectra of N 1 s indicates the binding energy at 398.78 eV, 400.62 eV and 402.78 eV, which are assigned to pyridinic nitrogen, pyrrolic nitrogen and graphitic nitrogen, respectively [12]. To access the affinity of ZG@Co with LiPS, the visual adsorption test was conducted

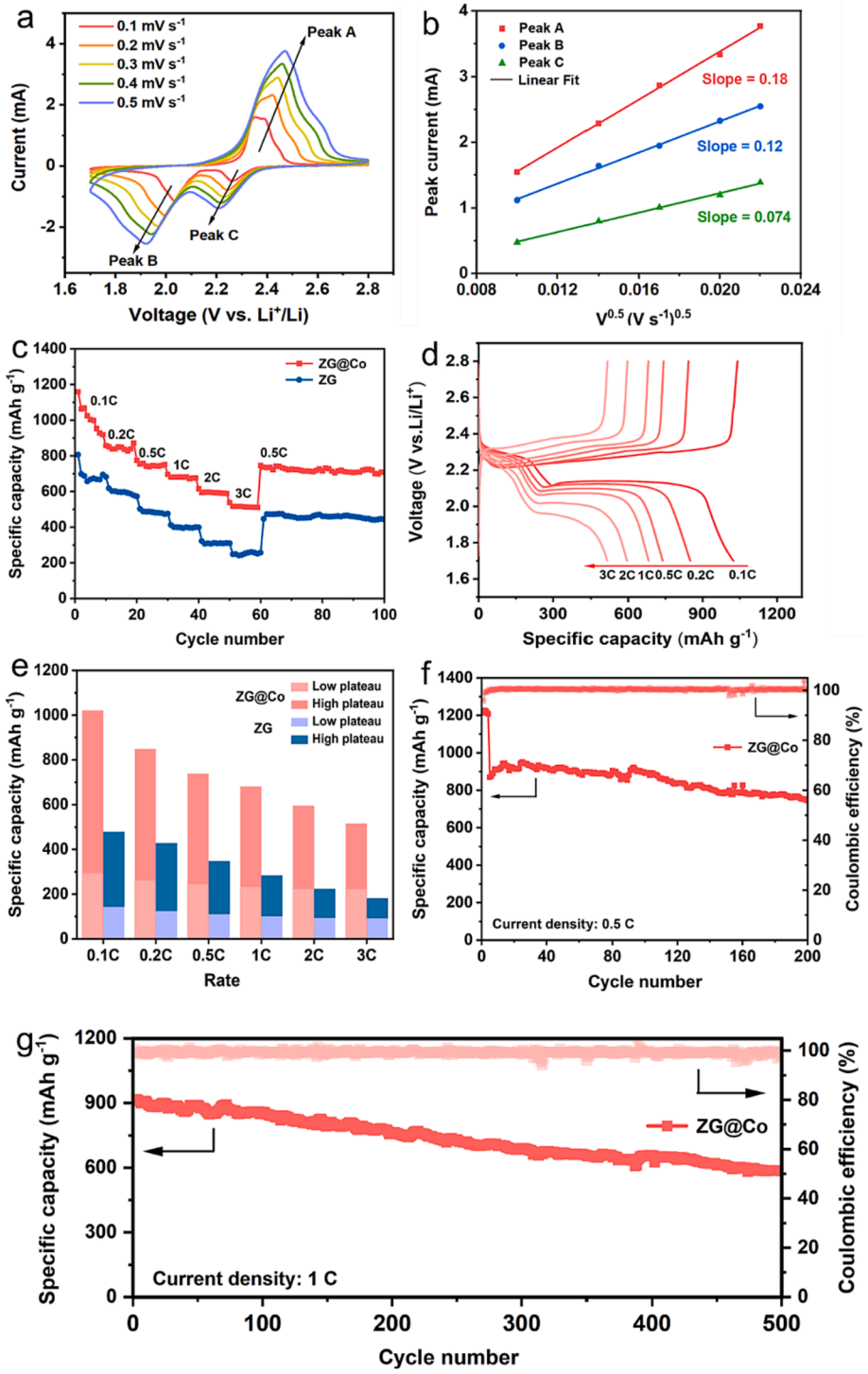

Fig. 3. (a) CV profiles of Li-S batteries with ZG@Co modified separator at a scan rate of 0.1–0.5 mV s^{-1} and (b) corresponding linear fits of the peak currents. (c) Rate capacity and (d) corresponding discharge/charge profiles of the cell with ZG@Co modified separator. (e) High plateau and low plateau discharge capacities for rate performance. Cycle performance of the cell with ZG@Co modified separator at (f) 0.5 C and (g) 1 C.

with the same amount of ZG and ZG@Co immersed into Li_2S_6 solution. After reacting for 12 h, the solution with ZG@Co becomes colorless (Fig. 2f), indicating a strong adsorption capacity for LiPSs. As shown in Fig. S4, after resting for 48 h cycled at 0.1 C, the battery based on ZG@Co system recovered initial capacity while a capacity of 84.5 mAh g ^{1} was lost in ZG system, further indicating that the shuttling effect of polysulfides on the ZG@Co modified separator is prohibited. Besides, symmetric cells were assembled in order to reveal the catalytic effect of different materials on the LiPSs redox reactions. The CV curve of ZG@Co symmetrical cell shows a larger current than ZG (Fig. 2g), demonstrating superior electrocatalytic effect of ZG@Co on reducing polarization and promoting LiPS conversions. As shown in Fig. 2h, i, the ZG@Co also exhibits a larger Li_2S nucleation capacity (210.74 mAh g ^{1}) than ZG (175.57 mAh g ^{1}), indicating a higher catalytic efficiency and faster redox kinetic towards Li_2S nucleation.

To verify the above properties for Li-S batteries, the electrochemical tests were examined with ZG@Co accelerator. The CV curves at different scan rates were measured to explore the Li^+ diffusivity (Fig. 3a). As

shown in Fig. 3b, the anodic and cathodic peak currents display a linear relationship with the square root of the scan rate, which denotes a diffusion-limited reaction. The electrochemical performances of battery with ZG@Co modified separator was further evaluated. Fig. 3c exhibits the distinctive charge–discharge plateaus and high discharge capacity as the current rate gradually increased to 3 C, indicating the fast LiPS reaction kinetics with the help of ZG@Co (Fig. 3d-e). Besides, the cell with ZG@Co accelerator also exhibits excellent cycling performance at 0.5 C (748.6 mAh g^{-1} after 200 cycles, Fig. 3f) and 1 C (585.3 mAh g^{-1} after 500 cycles, Fig. 3g), superior to that of controlled cell.

4. Conclusions

In summary, 2D Co/N co-doped mesoporous carbon nanosheets were successfully synthesized by self-assemble and pyrolysis. Thanks to its unique structure, physical constraint and chemical catalytic capability towards LiPSs, the cells with ZG@Co accelerator exhibit good rate performance (511.2 mAh g^{-1} at 3 C) and a long cycle stability (585.3 mAh g^{-1} after 500 cycles at 1 C).

CRediT authorship contribution statement

Siyu Wu: Writing – original draft, Writing – review & editing, Methodology, Formal analysis. **Xiang Li:** Formal analysis, Methodology, Resources. **Xin Zhang:** Formal analysis. **Yongzheng Zhang:** Supervision, Funding acquisition. **Jian Wang:** Supervision, Funding acquisition. **Chunyin Shen:** Supervision, Funding acquisition. **Hongzhen Lin:** Supervision, Funding acquisition. **Yanli Wang:** Supervision, Funding acquisition. **Liang Zhan:** Supervision, Funding acquisition.

Declaration of Competing Interest

The authors declare that they have no known competing financial interests or personal relationships that could have appeared to influence the work reported in this paper.

Data availability

Data will be made available on request.

Acknowledgements

S. W. and X. L contributed equally to this work. This work was financially supported by the National Key R&D Program of China (2021YFA1201503), National Natural Science Foundation of China (Nos. 22075081, 21972164, 22279161), the Fundamental Research Funds for the Central Universities (JKD01231701), and the Natural Science Foundation of Jiangsu Province (BK 20210130). Dr. J. Wang thanks the fellowship awarded by the Alexander von Humboldt Foundation.

References

[1] A. Manthiram, S.H. Chung, C.X. Zu, Adv. Mater. 27 (2015) 1980–2006.
[2] D.G. Xiong, Z. Zhang, X.Y. Huang, Y. Huang, J. Yu, J.X. Cai, Z.Y. Yang, J. Energy Chem. 51 (2020) 90–100.
[3] M. Tian, F. Pei, M.S. Yao, Z.H. Fu, L.L. Lin, G.D. Wu, G. Xu, H. Kitagawa, X.L. Fang, Energy Stor. Mater. 21 (2019) 14–21.
[4] H.L. Yang, Y.J. Lei, Q.R. Yang, B.W. Zhang, Q.F. Gu, Y.X. Wang, S.L. Chou, H. K. Liu, S.X. Dou, Electrochim. Acta 439 (2022), 141652.
[5] J.H. Wang, L.L. Gao, J.J. Zhao, J.D. Zheng, J. Wang, J.R. Huang, Mater. Res. Bull. 133 (2021), 111061.
[6] Y.Z. Zhang, G.X. Xu, Q. Kang, L. Zhan, W.Q. Tang, Y.X. Yu, K.L. Shen, H.C. Wang, X. Chu, J.Y. Wang, S.L. Zhao, Y.L. Wang, L.C. Ling, S.B. Yang, J. Mater. Chem. A 28 (2019) 16812–16820.
[7] Z.J. Cao, Y.Z. Zhang, Y.L. Cui, B. Li, S.B. Yang, Tungsten 2 (2020) 162–175.
[8] J. Xu, S.H. An, X.Y. Song, Y.J. Cao, N. Wang, X. Qiu, Y. Zhang, J.W. Chen, X. L. Duan, J.H. Huang, W. Li, Y.G. Wang, Adv. Mater. 33 (2021) 2105178.
[9] Z.J. Cao, Y.Z. Zhang, Y.L. Cui, J.N. Gu, Z.G. Du, Y.Z. Shi, K. Shen, H. Chen, B. Li, S. B. Yang, Energy Environ. Mater. 5 (2022) 45–67.
[10] C.Y. He, J.Z. Tao, Adv. Sustain. Syst. 2 (2018) 1700136.
[11] W.J. Wang, M.W. Liang, Y. Jiang, C.Y. Liao, Q. Long, X.F. Lai, L. Liao, Mater. Lett. 293 (2021), 129702.
[12] J.H. Wu, S.Y. Wang, Z.W. Lei, R.N. Guan, M.Q. Chen, P.W. Du, Y.L. Lu, R.G. Cao, S. F. Yang, Nano Res. 14 (2021) 2596–2605.